RESEARCH ARTICLE

Regional sea level change in response to ice mass loss in Greenland, the West Antarctic and Alaska

S.-E. Brunnabend[1,2], J. Schröter[1], R. Rietbroek[2], and J. Kusche[2]

[1]Alfred-Wegener-Institut, Helmholtz-Zentrum für Polar- und Meeresforschung, Climate Science Department, Division Climate Dynamics, Bremerhaven, Germany, [2]University of Bonn, Institute for Geodesy and Geoinformation, Department of APMG, Bonn, Germany

Abstract Besides the warming of the ocean, sea level is mainly rising due to land ice mass loss of the major ice sheets in Greenland, the West Antarctic, and the Alaskan Glaciers. However, it is not clear yet how these land ice mass losses influence regional sea level. Here, we use the global Finite Element Sea-ice Ocean Model (FESOM) to simulate sea surface height (SSH) changes caused by these ice mass losses and combine it with the passive ocean response to varying surface loading using the sea level equation. We prescribe rates of fresh water inflow, not only around Greenland, but also around the West Antarctic Ice Sheet and the mountain glaciers in Alaska with approximately present-day amplitudes of 200, 100, and 50 Gt/yr, respectively. Perturbations in sea level and in freshwater distribution with respect to a reference simulation are computed for each source separately and in their combination. The ocean mass change shows an almost globally uniform behavior. In the North Atlantic and Arctic Ocean, mass is redistributed toward coastal regions. Steric sea level change varies locally in the order of several centimeters on advective time-scales of decades. Steric effects to local sea level differ significantly in different coastal locations, e.g., at North American coastal regions the steric effects may have the same order of magnitude as the mass driven effect, whereas at the European coast, steric effects remain small during the simulation period.

1. Introduction

Beside global mean sea level change, or more specifically, the increase in the volume and mass of seawater, regional deviations from global mean sea level are of particular interest for an observer at the coast [*Cazenave et al.*, 2008; *Church and White*, 2011]. Furthermore, tide gauges are sensitive to relative sea level. It consists of changes in sea surface height (SSH) and vertical land motion of the land. The latter is may be influenced by a mixture of ongoing global isostatic adjustment (GIA), plate tectonics, subsidence of land due to the withdrawal of ground water or oil and gas, or the compaction of sediments [*Bindoff et al.*, 2007]. Additionally, mass loss of land ice causes mass distribution changes on the Earth's surface with an associated elastic response in uplift and geoid height. In the past five decades, a major contribution to sea level rise has originated from the expansion of water caused by warming of the ocean [*Levitus et al.*, 2005; *Gouretski and Koltermann*, 2007; *Gregory et al.*, 2013]. In addition, in recent decades, the major ice sheets in Greenland and West Antarctica have experienced increasing ice mass losses of hundreds of gigatons per year [e.g., *Rignot et al.*, 2008; *Wu et al.*, 2010; *Jacob et al.*, 2012; *Gregory et al.*, 2013, and others]. Furthermore, glaciers and ice-caps are melting [*Bindoff et al.*, 2007; *Gregory et al.*, 2013]. In conclusion, ocean warming and land ice mass loss are both of major importance when investigating sea level change in the global ocean.

To estimate the amount of mass loss of the ice sheets and glaciers, several studies have been performed using different techniques ranging from ice sheet modeling to satellite gravimetry and altimetry [*Wouters et al.*, 2008; *Gunter et al.*, 2009; *Jacob et al.*, 2012; *Velicogna et al.*, 2014; *Williams et al.*, 2014; *Schoen et al.*, 2015, and others]. During the last decade, many studies indicate a mass loss between 100 and 150 Gt/yr of West Antarctic Ice Sheet [*Vaughan et al.*, 2013; *Rignot et al.*, 2008; *Chen et al.*, 2009; *Wu et al.*, 2010; *Jacob et al.*, 2012; *Velicogna et al.*, 2014; *Schoen et al.*, 2015; *van der Wal et al.*, 2015], which is strongly dependent on the used GIA correction [*Whitehouse et al.*, 2012]. Regarding the Greenland Ice Sheet, an ice mass loss in the range of up to 278 Gt/yr has been estimated for the last decade [*Vaughan et al.*, 2013; *Luthcke et al.*, 2006; *Wouters et al.*, 2008; *Wu et al.*, 2010; *Jensen*, 2010; *Bamber*, 2012; *Jacob et al.*, 2012; *Schrama et al.*, 2014; *Velicogna et al.*, 2014],

which results in about 7 mSv of additional freshwater inflow (1 mSv = 1000 m^3/s). In case of the glaciers in Alaska, a mass loss rate of about 50 Gt/yr has been estimated [*Arendt et al.*, 2002; *Tamisiea et al.*, 2005; *Luthcke et al.*, 2008; *Berthier et al.*, 2010; *Jacob et al.*, 2012].

These losses of land ice mass induce a rise in global mean sea level, due to the additional freshwater mass. Furthermore, the mass redistribution leads to a change of the geoid height and crustal deformation affecting regional sea level [*Farrell and Clark*, 1976; *Francis and Mazzega*, 1990; *Mitrovica et al.*, 2001, and others]. Moreover, regional sea level is influenced by the freshening of seawater in the vicinity of the source region of the freshwater. It reduces the density and increases the specific volume, resulting in regional sea level rise. In addition to that, regional sea level responds to freshwater inflow due to changes in ocean circulation. As is done in this study, these dynamic sea level changes can be simulated using ocean models.

Several oceans model studies have been performed based on a variety of mass loss scenarios. An example is presented by *Gerdes et al.* [2006], who have analyzed the change of dynamic sea level change from Greenland ice mass loss by changing the surface boundary conditions in ocean general circulation models. The additional freshwater was converted into additional rain and spread along the coasts of Greenland. This technique is generally denoted as "hosing." *Gerdes et al.* [2006] found a reduced convection in the Labrador Sea. In addition, the weakened deep western boundary current transported more saline water. The study showed a strong sensitivity of the model results to the choice of the different boundary conditions. They also identified uncertainties resulting from the missing atmospheric response in ocean-only models.

When ocean circulation changes, oceanic temperature is advected differently. Thus the air-sea temperature difference is altered affecting surface heat fluxes. The atmospheric feedbacks, indirectly induced by continental ice mass loss and the associated variations at the ocean's surface, have been studied using a coupled atmosphere-ocean models. *Stammer et al.* [2011] compared the response of the ocean computed with an ocean-only model [*Stammer*, 2008] and a coupled model. They investigated the response to Greenland Ice Sheet mass loss during a 50 year simulation period and in the coupled model they found the existence of far field signals in the Indian and Pacific Ocean, which have not been visible in previous studies [e.g., *Gerdes et al.* 2006].

Weijer et al. [2012] showed that the spatial resolution is important when simulating the freshwater transport in the ocean. For example, they identified an increase in the velocity of the freshwater transport in the North Atlantic when using an eddy-resolving ocean model.

Wang et al. [2012] investigated the future ocean response to mass loss of the Greenland Ice Sheet in a water hosing experiment using the FESOM model. They simulated sea level and ocean circulation changes that are caused by a discharge rate of 0.1 Sv over 120 model years. Their results concentrate mainly on the consequences to meridional heat transport and vertical overturning caused by additional freshwater fluxes. They found a weakening of the AMOC strength and of its decadal variability.

Brunnabend et al. [2012] investigated the response of ocean circulation and the steric contribution to the regional sea level caused by mass loss of the Greenland Ice Sheet using the FESOM model. In that study, the associated steric contribution had only a small influence on global mean sea level rise, as shown before by *Munk* [2003] and *Lowe and Gregory* [2006]. On the other hand, the steric contribution led to strong regional deviations. A pattern was identified in the North Atlantic, which changed over time as the freshwater was distributed over the North Atlantic and the Arctic Ocean after 50 model years. The amount of the additional freshwater inflow around Greenland influenced the amplitude of the signal. However, it had only a small influence on the structure of the pattern, which may change when the additional mass loss would become high enough to alter the ocean circulation pattern [*Brunnabend et al.*, 2014].

The response to uplift and geoid change, including rotational feedback effects, caused by mass redistribution (in the following denoted as the static-equilibrium sea level response) was investigated in a water hosing experiment by [*Kopp et al.*, 2010] in addition to the sea level response due to the freshening and the changes in ocean circulation. A Greenland ice mass loss of 0.1 Sv was uniformly added to ocean surface in the North Atlantic. They found that dynamic sea level change has become significant at mass loss rates stronger than detected currently. Static-equilibrium sea level change becomes dominant in most ocean regions, except for the western North Atlantic, where freshwater contribution exceeded about 20 cm equivalent sea level.

While most hosing experiments apply high mass loss rates (e.g., 0.1 Sv) around Greenland, this study applies mass loss rates that are representative for the last decade (i.e., 7 mSv or 200 Gt/yr) in the simulation

experiments using a global configuration of the finite element sea-ice ocean model (FESOM) [*Wang et al.*, 2014; *Brunnabend et al.*, 2011]. Here, in addition to the investigation of the sea level response to the mass loss of the Greenland Ice Sheet, we also investigate the sea level response to the mass loss of the West Antarctic Ice Sheet and the glaciers in Alaska. The mass loss rates are assumed to be constant over time and are included during predefined mass loss seasons in the model simulations. The simulations are performed by applying each source of freshwater separately and in their combination. In addition, sea level change due to variations in gravitational attraction and the ocean floor deformation corresponding to ice mass loss, as well as the rotational effects of the mass redistribution are estimated and added to the modeled dynamic sea level change.

2. Data and Methods

2.1. Model Setup and Experiments

Monthly mean dynamic sea level change is calculated using the finite element sea-ice ocean model FESOM [*Wang et al.*, 2014; *Brunnabend et al.*, 2011]. The model is discretized on a global tetrahedral grid using the same mesh as applied in the study of *Sidorenko et al.* [2011], i.e., an unstructured and rotated mesh where the poles are located on land (Greenland and Antarctica). The model applies the set of primitive equations for oceanic motion including a fully nonlinear-free surface. The horizontal resolution ranges from 20 km near the coast and around Greenland to approximately 150 km in the open ocean. The high horizontal resolution resolves the boundary currents, which are important for the modeling of the freshwater transport. The vertical discretization is performed on 39 z-levels of varying thickness. The model does not account for ocean tides. Instead, it includes M2 tidal mixing formulation derived from the tpxo07 tide model of *Egbert and Erofeeva* [2002]. FESOM is initialized by using the temperature and salinity data of the World Ocean Atlas (WOA01) [*Stephens et al.*, [2002] and has a spin-up time period of 52 years (1958–2010) using NCEP forcing. The model is then run for one repeated period of 50 years (1960–2010), which defines the time period of the reference simulation as well as of the simulations that include additional freshwater inflows. A time step of 45 min is used.

The simulations performed in this study are forced with atmospheric data sets from the daily NCAR/NCEP reanalysis [*Kalnay et al.*, 1996]. The global mean ocean mass variations are directly linked to the freshwater fluxes from precipitation and evaporation prescribed by the NCAR/NCEP reanalysis and to the daily river runoff, provided by the land surface discharge model (LSDM) [*Dill*, 2008]. The freshwater flux is modeled as a flux of volume and mass but not of salt. Heat fluxes are calculated with bulk formulae [*Wang et al.*, 2014; *Timmermann et al.*, 2009] using daily mean shortwave and longwave radiation flux, 2 m temperature, and 2 m specific humidity of NCAR/NCEP reanalysis [*Kalnay et al.*, 1996]. No salinity or temperature restoring is used. The model applies the Boussinesq approximation, which conserves volume rather than mass. Hence, a sea level adjustment after Greatbatch [*Greatbatch*, 1994] is implemented to ensure conservation of mass.

Thermosteric expansion and halosteric contraction (steric height change) are accounted for by using the equation of state of *Jackett and McDougall* [1995] and added to modeled sea level change within the ocean model. However, modeled global mean thermosteric expansion amounts to about 1.2 mm/yr during the period 1970–2010 and approximately 2 mm/yr after 1993. These values are larger than the estimates of IPCC AR5 which are 0.8 and 1.1 mm/yr, respectively [*Church et al.*, 2013].

In this study, five experiments have been performed that differ from the reference run only by the additional input of freshwater, which is constant during the whole simulation period of 50 years (Table 1): (1) 200 Gt/yr of ice mass loss are converted to a volume flux and then equally distributed to all nodes along the coast of Greenland, which are located south of 75° north. (2) A freshwater inflow is included at the coast of the Gulf of Alaska corresponding to an ice mass loss of 50 Gt/yr. The changes in mass of all other mountain glaciers are not taken into account during this study as they are less localized. (3) A freshwater inflow equal to 100 Gt/yr of ice mass loss is applied to the West Antarctic coast. (4) The three mass loss scenarios described

Table 1. Hosing Experiments

Experiment	Areas of Ice Mass Loss	Rate (Gt/yr)
1	Greenland	200
2	Alaska Glaciers	50
3	West Antarctica	100
4	Greenland, Alaska Glaciers, West Antarctica	200, 50, 100
5	Greenland, West Antarctica	200, 100

above are combined in a model simulation, to investigate the linearity of regional sea level change caused by the different contributions. For the same reason, (5) the mass losses of only the Greenland and West Antarctic Ice Sheet are combined in a model simulation. In all simulations, it is assumed that for the northern hemisphere, freshwater inflow occurs from May to October and for the southern hemisphere from November to April. Changes in regional sea level are then computed by taking the difference between the reference model simulation and the respective simulation including additional freshwater inflow.

2.2. Static-Equilibrium Sea Level Change

The reduced ice masses in Greenland, the West Antarctic, and Alaska cause time-variable differences of the geoid, including rotational effects, minus the uplift of the ocean bottom. The sea level changes arising from the changing ice and ocean loads are computed using the sea level equation, which is solved in spectral domain using real-valued fully normalized spherical harmonic base functions [*Farrell and Clark*, 1976; *Rietbroek et al.*, 2012]. The unknown relative sea level is assumed to coincide with an equipotential surface, i.e., it is responds to the gravitational effects of the prescribed load on land, the associated rotational potential change, and the gravitational effects of the sea level itself [*Rietbroek et al.*, 2012]. The redistribution of mass between land ice and ocean, and within the ocean, leads to a small shift of the Earth's rotation axis. This leads to small changes in centrifugal potential that, in turn, create a small but large-scale change in sea level. When solving for the static equilibrium response, we use loading Love numbers from the PREM Earth model [*Dziewonski*, 1981] to model the Earth's deformation response to surface loading, and the associated geoid response.

The linear behavior of the sea level equation allows to superimpose the sea level contributions from the major ice sheets and Alaskan glaciers. Therefore, to the mass loss of the major ice sheet and the Alaska Glaciers, which are constructed for signals representative for the last decade. Here, a time-invariant ocean function is assumed as it is expected that the shoreline has not migrated by much during the time period of study. The patterns of the mass loss regions are taken from the database of *Rietbroek et al.* [2012], where the ice mass loss in Greenland is assumed as to be uniform over the entire Greenland Ice Sheet. The ice mass loss of the West Antarctic Ice Sheet is assumed to be uniform over the entire West Antarctic excluding the Antarctic Peninsula. The self-consistent sea level response to melting of the Alaskan glaciers is taken from *Rietbroek et al.* [2012].

In this study, the global mean sea level change has been subtracted from the static-equilibrium sea level change as it is already contained in the mass conserving ocean model. For more detailed information about the method, please refer to *Rietbroek et al.* [2012].
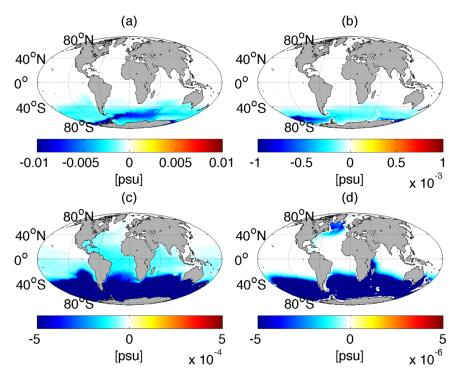
3. Results

3.1. Freshwater Distribution

The inflow of the additional freshwater is modeled as a flux of volume and mass which leads to a nonlinear response according to the equation of state for sea water. To study the path of the freshwater, a passive tracer is added to the inflow. This tracer is advected by the ocean dynamics in the same way as temperature and salinity (which are not passive tracers). The tracer distribution depicts the freshening of the ocean that is caused by the mass loss of the ice sheets. Figure 1 shows the freshwater distribution that originates from the West Antarctic Ice Sheet. The freshwater mainly stays in the region of the source, however, as soon as it reaches the Antarctic Circumpolar Current (ACC) it is distributed around the whole Antarctic continent. In addition, some freshwater flows west with the coastal current. After reaching the Ross Sea Gyre, most of it sinks into the deeper ocean. This water is subsequently distributed around the Antarctic continent at depth. Near the surface, some freshwater passes the ACC and is transported through surface currents to the north.

Figures 2a and 2b show the modeled passive tracer caused by the additional freshwater inflow near the coast of Greenland. These values describe the distribution of the freshwater leading to halosteric sea level rise. After 50 years (mean of year 50), the surface currents have transported the freshwater from Baffin Bay and the Labrador Sea southward along the North American coast, leaving some freshwater in Hudson Bay. Another part is transported via the subpolar gyre to the European coast where it separates into two branches flowing into the Arctic Ocean and along the subtropical gyre to the equatorial Atlantic Ocean. Some freshwater is also sinking to greater depths where it spreads southward along the American coast

Figure 1. Passive tracer corresponding to the reduced salinity (in psu), depicting the distribution of the freshwater inflow from the West Antarctic Ice Sheet at different depth (after 50 years): (a,c) surface, (b,d) 1500 m. Note the different color scale of the different plots (Figures 1a and 1b versus 1c and 1d) is used to show the signals in the Southern Ocean and the North Atlantic.
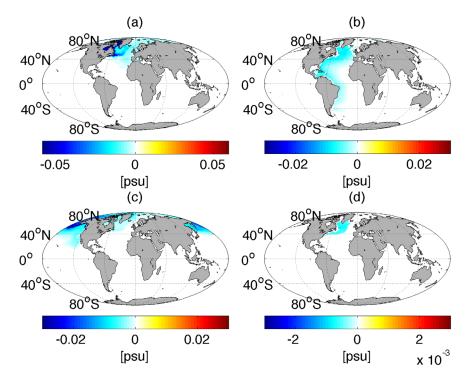

Figure 2. Passive tracer corresponding to the reduced salinity (in psu), depicting the distribution of the freshwater inflow along the coast of Greenland (a,b), and the Alaska Glaciers (c,d) at different depth (after 50 years): (Figures 2a and 2c) surface, (Figures 2b and 2d) 1500 m. Note the different color scale of the different plots.
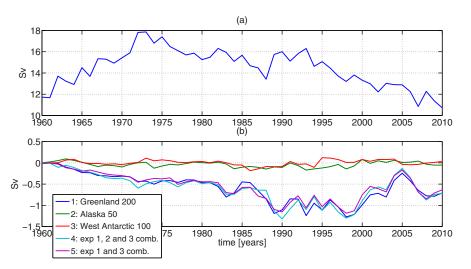
Figure 3. Maximum AMOC at 45N of (a) the control simulation and (b) the response to the additional freshwater inflow of the different experiments.

towards the South Atlantic Ocean. These results agree well with studies from *Gerdes et al.* [2006] and *Brunnabend et al.* [2012].

Figures 2c and 2d show the passive tracer of the reduced salinity caused by freshwater inflow from the Glaciers of Alaska. In this experiment, the freshwater is transported close to the surface to the Arctic Ocean through Bering Strait where it flows into the Beaufort Gyre and further into the North Atlantic Ocean. Only a small amount of freshwater is transported southward near the eastern coast of North America to equatorial regions. In addition, a small portion of the freshwater is directed to the equatorial Pacific Ocean.

3.2. Atlantic Meridional Overturning

The applied freshwater inflows caused by the mass loss of land ice have only small influence on the Atlantic meridional overturning circulation (AMOC).The maximum AMOC at 45°N is commonly used as an index to characterize the full overturning circulation. In the reference simulation, the mean strength of the yearly mean AMOC at 45°N is about 14.5 Sv (1 Sv $= 10^6$ m^3/s) with a variance of 3.1 Sv (Figure 3a). Only the results of the experiments, where the freshwater inflow of 200 Gt/yr around Greenland is included, show a significant difference (experiments 1, 4, and 5). A reduced salinity is slightly stabilizing the water column in the region of deep water formation. The AMOC slows down. Its maximum strength at 45°N slowly decreases by about 1 Sv with respect to the reference simulation within the first 30 years of the hosing period. Subsequently, it remains at the lower level with increased interannual variability (from 0.1 Sv to about 0.3 Sv). In the experiments including only freshwater inflow caused by the ice mass loss of the West Antarctic Ice Sheet or the glaciers in Alaska (experiment 2 and 3), the AMOC experiences almost no change as the amount of freshwater reaching the deep water formation areas is to small to initiate alterations in the water column. The AMOC remains at the same level as the reference simulation (Figure 3b). The difference with respect to the reference simulation only slightly varies by about 0.06 Sv.

However, the modeled AMOC results strongly depend on the model configuration. The strength of the AMOC is strongly influenced by the model parameterization and the spatial resolution used during the model experiments. In the study of *Brunnabend et al.* [2012], using a low-resolution model grid (1.5 × 1.5°), the AMOC was fairly weak and more freshwater could reach the equatorial Atlantic Ocean. In the present study, however, the AMOC is stronger and the freshwater spreads out more in the direction of the Arctic Ocean. Higher values (about 20 Sv at 45°N) are reached in the study of *Sidorenko et al.* [2009]. They used the finite-element ocean circulation model (FEOM) with a horizontal resolution ranging from 0.2 to 1° in the North Atlantic with highest resolution in the Gulf Stream area. Another difference to the model used here is that temperature and salinity are forced by relaxation to monthly mean sea surface temperature of the WOA01 climatology. Such a restoring is not applied here, as it would distort the results of the hosing experiments.
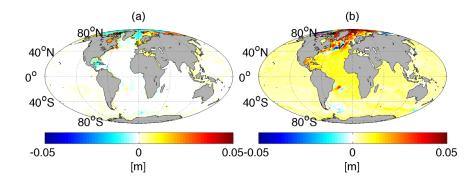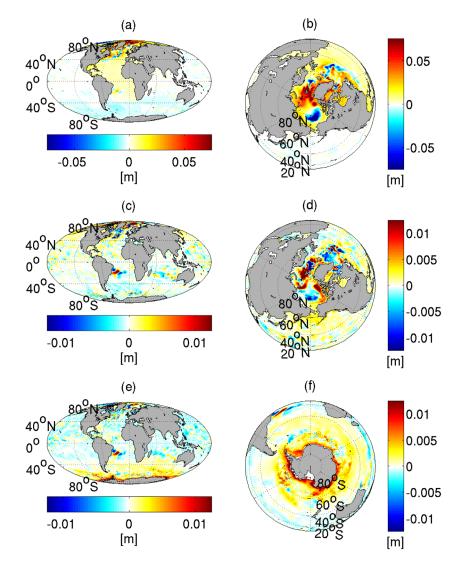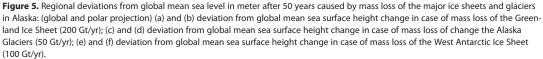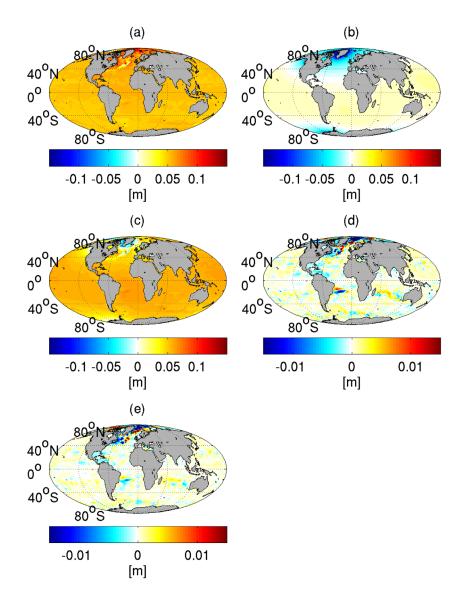
Figure 4. Modeled regional sea level change due to ice mass loss in meters after 50 years including all mass loss locations in the model simulation, separated into (a) ocean mass redistribution, where the global mean change of 5.1 cm is subtracted and (b) steric height change.

Figure 5. Regional deviations from global mean sea level in meter after 50 years caused by mass loss of the major ice sheets and glaciers in Alaska: (global and polar projection) (a) and (b) deviation from global mean sea surface height change in case of mass loss of the Greenland Ice Sheet (200 Gt/yr); (c) and (d) deviation from global mean sea surface height change in case of mass loss of change the Alaska Glaciers (50 Gt/yr); (e) and (f) deviation from global mean sea surface height change in case of mass loss of the West Antarctic Ice Sheet (100 Gt/yr).

Figure 6. Regional sea level change caused by mass loss of the major ice sheets and the Alaska Glaciers (after 50 years in meter): (a) modeled sea level change, including the mass loss in all three regions; (b) static-equilibrium sea level change; (c) regional sea level change (Figures 6a + 6b); (d) difference between modeled sea level change of the simulation considering the three contributors (shown in Figure 6a) and sea level change computed as sum of the three simulations considering the sources of mass loss separately; (e) difference between modeled sea level change of the simulation considering the contributors from Greenland and the West Antarctic and sea level change computed as sum of these two simulations considering the sources of mass loss separately.

3.3. Sea Level Change Caused by Land Ice Mass Loss

Beside the modeled global mean sea level change of about 0.6 mm/yr for a mass loss rate of 200 Gt/yr, mainly the steric contribution in the ocean leads to regional sea level change in the hosing experiments. Ocean circulation changes, caused by the applied mass loss rates, appear to be rather small. However, this may change with increasing land ice mass loss as for example stated by *Gregory et al.* [2003], *Stammer* [2008], *Stammer et al.* [2011], and *Brunnabend et al.* [2014]. Modeled sea level change that is induced by the land ice mass loss can be separated into its mass and steric contribution. After 50 years, the pattern of sea level change is partly associated to the small reduction of the AMOC [*Yin et al.*, 2009, 2010; *Kienert and Rahmstorf*, 2012], which causes a sea level rise at the northeast American coast due to redistribution of ocean mass (Figure 4a). The steric contribution (Figure 4b) is responsible for the complex pattern in the North Atlantic and Arctic Ocean caused by the additional freshwater and an atmospheric feedback changing the net heat flux between atmosphere and ocean.
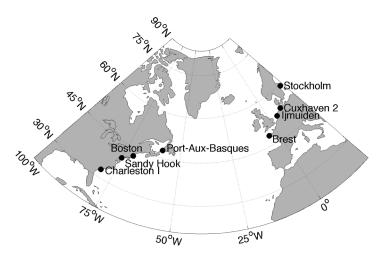
Figure 7. Locations at the North American and European coast.

Figure 5 shows the contributions to regional deviations from modeled global mean sea level of the different regions of ice mass loss. After 50 years, variations in modeled sea level are concentrated in the regions of freshwater inflow. In response to a Greenland Ice Sheet mass loss of 200 Gt/yr (Figures 5a and 5b), there are deviations from modeled global mean sea level visible which are mainly located in the North Atlantic and the Arctic Ocean (Figure 5a). The process of how the modeled sea level changes within FESOM under a Greenland mass loss scenario, is described in detail in the water-hosing experiment of *Wang et al.* [2012].

The freshwater distribution, resulting from the freshwater inflow in Alaska, also leads to a regional pattern of modeled sea level change in the North Atlantic Ocean (Figures 5c and 5d). But in contrast to the simulation including mass loss of the Greenland Ice Sheet, modeled sea level rise in the Arctic is located mainly in shallow regions north of Alaska and Canada corresponding to the flow path of the freshwater. In addition, the freshwater tongue in the equatorial Pacific does not lead to a clear signal in modeled sea level change.

As most freshwater remains in the Southern Ocean in the West Antarctic ice mass loss scenario, modeled sea level changes mainly occur in this region (Figures 5e and 5f). The modeled sea level rise near the source of ice mass loss is not as pronounced as in the Greenland hosing experiment, as only half as much ice mass is lost and is redistributed to a larger area in the Southern Ocean by the ACC. However, far field variations are also visible, e.g., in the North Atlantic (Figure 5e). These are caused by changes in the heat fluxes between atmosphere and ocean (not shown). Similar changes can be identified in the two experiments including the Alaska and Greenland mass loss scenario.

Figure 6a shows the modeled sea level change due to the combined mass loss of the two ice sheets and the glaciers of Alaska after 50 years including modeled global mean sea level change. Strong sea level change is found near the coast where the ice mass is lost. This especially holds for the Greenland coast where most freshwater flows into the ocean. The corresponding static-equilibrium sea level change (Figure 6b) decreases in the vicinity of the sources and slightly increases at greater distances. As pointed out by earlier studies [e.g., *Mitrovica et al.*, 2001], the decrease due to the static equilibrium change is larger than the modeled increase in steric height and modeled sea level now falls in the regions around Greenland. Near the coast of the West Antarctic Ice Sheet and the Alaska Glaciers, the sea level rise becomes lower than the global mean sea level change (Figure 6c).

One may wonder whether modeled sea level change of the simulation, including combined mass losses, and the sum of the three simulations, which consider the mass contributions separately, add up to the same effect. Figures 6d and 6e show that this is not the case. Here, differences up to ±3 cm mainly occur in the North Atlantic and the Arctic Ocean after 50 years. They arise as the different freshwater contributions interact with each other in the simulation using the combined ice mass loss. These interactions are not considered when simulating regional sea level change caused by the different sources separately. Hence, ocean circulation may react differently causing local differences in sea level. This also leads to different heat flux
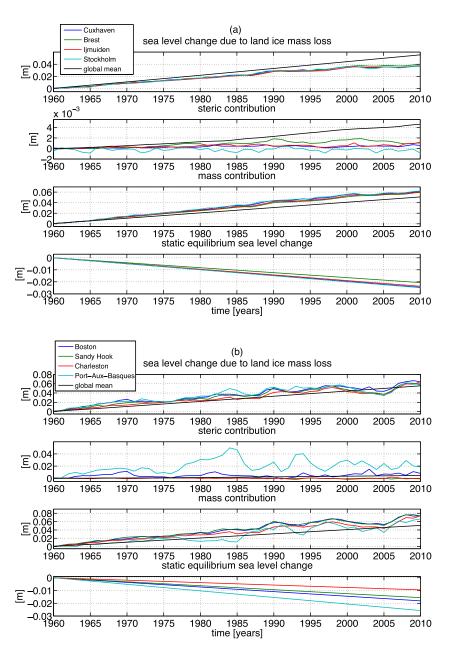
Figure 8. Modeled mass and steric contributions to sea level change and the static equilibrium sea level change caused by land ice mass loss at different coastal locations in the North Atlantic region: (a) European coast (b) North American coast.

between atmosphere and ocean, mainly responsible for the difference in the North Atlantic. The effects due to this nonlinearity are generally smaller than the regional sea level change but are nonetheless visible and therefore become important when investigating sea level change caused by land ice mass loss.

Sea level change at a number of coastal locations around the North Atlantic Ocean are chosen (Figure 7) where the impact of ice mass loss appeared most significant. Figures 8a and 8b show the change in sea level at different location at European and the North American coast, respectively. Signals from steric and mass contribution are separated. Additionally, the static-equilibrium sea level changes due to the land ice mass losses are shown. At the European coast, sea level is mainly influenced by the additional mass. The mass contribution in this coastal region is slightly higher than the global mean sea level change due the additional freshwater. On the other hand, the steric contribution is rather small. It is one order of magnitude smaller than the mass contribution. The static-equilibrium sea level change compensates the extra mass contribution leading to a regional sea level change lower than the global mean.

During the 50 years of the simulation experiments, sea level changes appears to be most of the time of about 2 cm above the global mean along the coast of Port-Aux-Basques, Canada (Figure 8b). In this region, the modeled steric contribution becomes stronger especially at the northern locations (e.g., at Port-Aux-Basques). Here the modeled steric contribution reaches about one third of the amplitude of the mass contribution. The modeled mass increase due to the change in circulation is also significant, outweighing the signal of the static-equilibrium sea level change. Although these locations are fairly close to the sources of the mass loss in Greenland, they are not near enough for this signal to dominate regional sea level change in this simulation. These might change when simulating with higher mass loss rates or applying a longer simulation time period.

4. Discussion and Conclusion

Besides the mass loss of the Greenland Ice Sheet, this study also includes ice mass loss of the West Antarctic Ice Sheet as well as the Alaskan Glaciers. It shows that rates of ice mass loss, which are one order of magnitude smaller than in previous studies, lead to a signal in regional deviations from modeled global mean sea level change in the order of several centimeters. The land ice mass loss in different regions lead to different signals in modeled regional sea level change with largest signals near its source. Here, the steric signal is dominant and are caused by the additional freshwater, whereas during the 50 years of the model simulations changes circulation patterns are rather small. Only the small reduction of the AMOC in the experiments including the mass loss of the Greenland Ice Sheet leads to a redistribution of mass towards the coast mainly in the North Atlantic and the Arctic Ocean.

Atmospheric feedbacks potentially play an important role in the North Atlantic since, depending on the forcing parameters, the heat exchange between ocean and atmosphere changes. *Stammer et al*. [2011] used a coupled model for simulating the ocean and atmospheric response to Greenland ice mass loss. They showed that changing the freshwater inflow around Greenland leads to atmospheric responses not only in regions where the additional freshwater accumulates but also in far distant regions such as the Indian Ocean. In addition, the strength of the AMOC is of major importance when simulating the meridional heat transport. This heat transport reacts very sensitive to the changes in the AMOC [*Stammer et al*., 2011] and was reduced to a very low level. The results of *Stammer et al*. [2011] indicate that also coupled models are very sensitive to their parameterization, and that different models might react differently. For example, the model setup used in the study of *Gerdes et al*. [2006] shows less impact. For these reason, it would be desirable to have more sensitivity studies using coupled atmosphere-ocean models and uncoupled ocean models. It should be noted that, for our study, atmospheric fields and fluxes from a reanalysis are used, which include quite an amount of data assimilation. Therefore, most of the real feedback of the atmosphere ocean system over the past 50 years is already accounted for in our experiments.

Static-equilibrium sea level change caused by the redistribution of the ice mass may have the same order of magnitude compared to the steric sea level response and the change due to different ocean circulation. Our findings support the study of *Kopp et al*. [2010] stating that the anomalies get locally dominant with higher mass loss rates. In addition, this might be also true when investigating longer time series. The pattern of the static-equilibrium sea level response remains constant over time. However, sea level changes due to the response of freshwater inflow vary regionally and in time as ocean circulation may change and the freshwater is transported to regions that are farther away from the origin of the freshwater source.

Differences to reality may also be caused by our approximations of the melting rates and locations in this study. Possibly, not as much ice mass was lost during the first decades of the simulations as in the last decades [*Lemke et al*., 2007] and recent ice mass loss in Greenland is well above our applied rate [*Schrama et al*., 2014]. Beside sediment compaction and vertical land movement caused by earthquakes and/or local GIA, also the contributions of the mountain glaciers and other hydrological sources are not accounted for here.

To improve the current study, several advances can be made. Geodetic observations of ice mass loss may be used as improved input parameters in the model. Furthermore, the sea level contributions from mountain glaciers need to be taken into account. In possible future studies, modeled sea level change caused by ocean warming, including the deep ocean, may be investigated. Also it is beneficial to increase the horizontal in the open ocean, e.g., to model a more realistic AMOC that may change the dynamic sea level response due to the additional freshwater as shown e.g., by *Weijer et al*. [2012].

References

Arendt, A. A., K. A. Echelmeyer, W. D. Harrison, C. S. Lingle, and V. B. Valentine (2002), Rapid Wastage of Alaska Glaciers and their Contribution to Rising Sea Level, *Science*, *297*, 382–386.

Bamber, J. (2012), Shrinking glaciers under scrutiny, *Nature*, *482*, 482–483.

Berthier, E., E. Schiefer, G. K. C. Clarke, B. Menounos, and F. Remy (2010), Contribution of Alaskan glaciers to sea-level rise derived from satellite imagery, *Nat. Geosci.*, *3*, 92–95, doi:10.1038/ngeo737.

Bindoff, N. L., et al. (2007), Observations: Oceanic climate change and sea level, in *The Scientific Basis, Contribution of Working Group I to the Fourth Assessment Report of the Intergovernmental Panel on Climate Change*, edited by S. Solomon, et al., pp. 385–432, Cambridge Univ. Press, Cambridge, N. Y.

Brunnabend, S.-E., R. Rietbroek, R. Timmermann, J. Schröter, and J. Kusche (2011), Improving mass redistribution estimates by modeling ocean bottom pressure uncertainties, *J. Geophys. Res.*, *116*, C08037, doi:10.1029/2010JC006617.

Brunnabend, S.-E., J. Schröter, R. Timmermann, R. Rietbroek, and J. Kusche (2012), Modeled steric and mass-driven sea level change caused by Greenland Ice Sheet melting, *J. Geodyn.*, *59*(60), 219–225, doi:10.1016/j.jog.2011.06.001.

Brunnabend, S.-E., H. A. Dijkstra, M. A. Kliphuis, B. van Werkhoven, H. E. Bal, F. Seinstra, J. Maassen, and M. van Meersbergen (2014), Changes in extreme regional sea surface height due to an abrupt weakening of the Atlantic meridional overturning circulation, *Ocean Sci.*, *10*, 881–891, doi:10.5194/os-10-881-2014.

Cazenave, A., A. Lombard, and W. Llovel (2008), Present-day sea level rise: A synthesis, *C. R. Geosci.*, *340*, 761770, doi:10.1016/j.crte.2008.07.008.

Chen, J. L., C. R. Wilson, D. Blankenship, and B. Tapley (2009), Accelerated antarctic ice loss from satellite gravity measurements, *Nat. Geosci.*, *2*, 859–862, doi:10.1038/ngeo694.

Church, J. A., and N. J. White (2011), *Sea-level rise from the Late 19th to the Early 21st Century*, *Surv. Geophys.*, *32*, 585602, doi:10.1007/s10712-011-9119-1.

Church, J. A., et al. (2013), Sea level change, in *The Scientific Basis, Contribution of Working Group I to the Fifth Assessment Report of the Intergovernmental Panel on Climate Change*, edited by T. F. Stocker et al., pp. 1137–1216, Cambridge Univ. Press, Cambridge, U. K.

Dill, R. (2008), Hydrological model LSDM for operational Earth rotation and gravity field variations, (Scientific Technical Report STR; 08/09), Potsdam : Deutsches GeoForschungsZentrum GFZ, 35 S.: Ill., graph. Darst. p. doi:10.2312/GFZ.b103-08095.

Dziewonski, A. (1981), Preliminary reference earth model, *Phys. Earth Planet. Int.*, *25* (4), 297–356, doi:10.1016/0031-9201(81)90046-7.

Egbert, G., and S. Erofeeva (2002), Efficient inverse modeling of barotropic ocean tides, *J. Atmos. Oceanic Technol.*, *19*, 183–204.

Farrell, W. E., and J. A. Clark (1976), On postglacial sea level, *Geophys. J. R. Astron. Soc.*, *46*, 647–667.

Francis, O., and P. Mazzega (1990), Global charts of ocean tide loading effects, *J. Geophys. Res.*, *95*, 411–424.

Gerdes, R., W. Hurlin, and S. M. Griffies (2006), Sensitivity of a global ocean model to increased run-off from Greenland, *Ocean Modell.*, *12*(3–4), 416–435, doi:10.1016/j.ocemod.2005.08.003.

Gouretski, V., and K. P. Koltermann (2007), How much is the ocean really warming, *Geophys. Res. Lett.*, *34*, L01610, doi:10.1029/2006GL027834.

Greatbatch, R. J. (1994), A note on the representation of steric sea level in models that conserve volume rather than mass, *J. Geophys. Res.*, *99*, 12,767–12,771.

Gregory, J. M., O. A. Saenko, and A. J. Weaver (2003), The role of the Atlantic freshwater balance in the hysteresis of the meridional overturning circulation, *Clim. Dyn.*, *21*, 707–717, doi:10.1007/s00382-003-0259-8.

Gregory, J. M., et al. (2013), Twentieth-century global-mean sea-level rise: Is the whole greater than the sum of the parts?, *J. Clim.*, *26*, 4476–4499, doi:10.1175/JCLI-D-12-00319.1.

Gunter, B., T. Urban, R. Riva, M. Helsen, R. Harpold, S. Poole, P. Nagel, B. Schutz, and B. Tapley (2009), A comparison of coincident GRACE and ICESat data over Antarctica, *J. Geod.*, *34*, 1051–1060, doi:10.1007/s00190-009-0323-4.

Jackett, D., and T. J. McDougall (1995), Stabilization of hydrographic data, *J. Atmos. Oceanic Technol.*, *12*, 381–389.

Jacob, T., J. Wahr, W. T. Pfeffer, and S. Swenson (2012), Recent contribution of glaciers and ice caps to sea level rise, *Nature*, *482*, 514–518, doi:10.1038/nature10847.

Jensen, L. (2010), Schätzung der Eismassenbilanz von Grönland mit Hilfe von GRACE und komplementären Daten, MS thesis, Univ. Bonn, Germany.

Kalnay, E., et al. (1996), The NCEP/NCAR 40-year reanalysis project, *Bull. Am. Meteorol. Soc.*, *77*, 437–471.

Kienert, H., and S. Rahmstorf (2012), On the relation between meridional overturning circulation and sea-level gradients in the Atlantic, *Earth Syst. Dyn.*, *3*, 109–120, doi:10.5194/esd-3-109-2012.

Kopp, R. E., J. X. Mitrovica, S. M. Griffies, J. Yin, C. C. Hay, and R. J. Stouffer (2010), The impact of Greenland melt on local sea levels: A partially coupled analysis of dynamic and static equilibrium effects in idealized water-hosing experiments, *Clim. Change*, *103*, 619–625, doi:10.1007/s10584-010-9935-1.

Lemke, P., et al. (2007), Observations: Changes in snow, ice and frozen ground, in *Climate Change 2007: The Physical Science Basis. Contribution of Working Group I to the Fourth Assessment Report of the Intergovernmental Panel on Climate Change*, edited by S. Solomon et al., pp. 337–383, Cambridge Univ. Press, Cambridge, N. Y.

Levitus, S., J. I. Antonov, and T. P. Boyer (2005), Warming of the world ocean, 1995-2003, *Geophys. Res. Lett.*, *32*, L02604, doi:10.1029/2004GL021592.

Lowe, J. A., and J. M. Gregory (2006), Understanding projections of sea level rise in a Hadley Centre coupled climate model, *J. Geophys. Res.*, *11*, C11014, doi:10.1029/2005JC003421.

Luthcke, S. B., et al. (2006), Recent Greenland Ice mass loss by drainage system from satellite gravity observations, *Science*, *314*, 1286–1289, doi:10.1126/science.1130776.

Luthcke, S. B., A. A. Arendt, D. D. Rowlands, J. J. M. Carthy, and C. F. Larsen (2008), Recent glacier mass changes in the gulf of Alaska region from grace mascon solutions, *J. Glaciol.*, *54*, 767–777.

Mitrovica, J. X., M. E. Tamisiea, J. L. Davis, and G. A. Milne (2001), Recent mass balance of polar ice sheets inferred from patterns of global sea-level change, *Nature*, *409*, 1026–1029.

Munk, W. (2003), Ocean freshening, sea level rising, *Science*, *300*, 2041–2043, doi:10.1126/science.1085534.

Rietbroek, R., S.-E. Brunnabend, J. Kusche, and J. Schröter (2012), Resolving sea level contributions by identifying fingerprints in time-variable gravity and altimetry, *J. Geodyn.*, *59-60*, 72–81, doi:10.1016/j.jog.2011.06.007.

Rignot, E., J. L. Bamber, M. R. van den Broeke, C. D. Y. Li, W. J. van de Berg, and E. V. Meijgaard (2008), Recent Antarctic ice mass loss from radar interferometry and regional climate modelling, *Nat. Geosci.*, *1*, 106–110, doi:10.1038/ngeo102.

Schoen, N., A. Zammit-Mangion, J. C. Rougier, T. Flament, F. Remy, S. Luthcke, and J. L. Bamber (2015), Simultaneous solution for mass trends on the West Antarctic Ice Sheet, *The Cryosphere*, *9*, 805–819, doi:10.5194/tc-9-805-2015.

Schrama, E., B. Wouters, and R. Rietbroek (2014), A mascon approach to assess ice sheet and glacier mass balances and their uncertainties from GRACE data., *J. Geophys. Res. Solid Earth*, *119*, 6048–6066, doi:10.1002/2013JB010923.

Sidorenko, D., S. Danilov, Q. Wang, A. Huerta-Casas, and J. Schröter (2009), On computing transports in finite-element models, *Ocean Model.*, *28*(1), 60–65, doi:10.1016/j.ocemod.2008.09.001.

Sidorenko, D., Q. Wang, S. Danilov, and J. Schröter (2011), FESOM under coordinated ocean-ice reference experiment forcing, *Ocean Dyn.*, *61*, 881–890, doi:10.1007/s10236-011-0406-7.

Stammer, D. (2008), Response of the global ocean to Greenland and Antarctic ice melting, *J. Geophys. Res.*, *113*, C06022, doi:10.1029/2006JC004079.

Stammer, D., N. Agarwal, P. Herrmann, A. Köhl, and C. R. Mechoso (2011), Response of a coupled ocean-atmosphere model to Greenland ice melting, *Surv. Geophys.*, *32*, 621–642, doi:10.1007/s10712-011-9142-2.

Stephens, C., J. I. Antonov, T. P. Boyer, M. E. Conkright, R. Locarnini, and T. D. O'Brien (2002), *World Ocean Atlas 2001, NOAA Atlas NESDID 49*, U.S. Govt. Print. Off., Washington, D. C.

Tamisiea, M. E., E. W. Leuliette, J. L. Davis, and J. X. Mitrovica (2005), Constraining hydrological and cryospheric mass flux in southeastern Alaska using space-based gravity measurements, *Geophys. Res. Lett.*, *32*, L20501 doi:10.1029/2005GL023961.

Timmermann, R., S. Danilov, J. Schröter, C. Böning, D. Sidorenko, and K. Rollenhagen (2009), Ocean circulation and sea ice distribution in a finite-element global sea ice: Ocean model, *Ocean Modell.*, *27*, 114–129, doi:10.1016/j.ocemod.2008.10.009.

van der Wal, W., P. L. Whitehouse, and E. J. Schrama (2015), Effect of GIA models with 3D composite mantle viscosity on GRACE mass balance estimates for Antarctica, *Earth Planet. Sci. Lett.*, *414*, 134–143, doi:10.1016/j.epsl.2015.01.001.

Vaughan, D., et al. (2013), Observations: Cryosphere, in *Climate Change 2013: The Physical Science Basis. Contribution of Working Group I to the Fifth Assessment Report of the Intergovernmental Panel on Climate Change*, edited by T. Stocker et al., Cambridge Univ. Press, Cambridge, U. K.

Velicogna, I., T. C. Sutterley, and M. R. van den Broeke (2014), Regional acceleration in ice mass loss from Greenland and Antarctica using GRACE time-variable gravity data, *Geophys. Res. Lett.*, *41*, 8130–8137, doi:10.1002/2014GL061052.

Wang, Q., S. Danilov, D. Sidorenko, R. Timmermann, C. Wekerle, X. Wang, T. Jung, and J. Schröter (2014), The Finite Element Sea Ice-Ocean Model (FESOM) v.1.4: Formulation of an ocean general circulation model, *Geosci. Model Dev.*, *7*(2), 663–693, doi:10.5194/gmd-7-663-2014.

Wang, X., Q. Wang, D. Sidorenko, S. Danilov, J. Schröter, and T. Jung (2012), Long term ocean simulations in FESOM: Validation and application in studying the impact of Greenland Ice Sheet melting, *Ocean Dyn.*, *62*(10), pp. 1471–1486, doi:10.1007/s10236-012-0572-2.

Weijer, W., M. E. Maltrud, M. W. Hecht, H. A. Dijkstra, and M. A. Kliphuis (2012), Response of the Atlantic Ocean circulation to Greenland Ice Sheet melting in a strongly-eddying ocean model, *Geophys. Res. Lett.*, *39*, L09606, doi:1029/2012GL051611.

Whitehouse, P. L., M. J. Bentley, G. A. Milne, M. A. King, and I. D. Thomas (2012), A new glacial isostatic adjustment model for Antarctica: Calibrated and tested using observations of relative sea-level change and present-day uplift rates, *Geophys. J. Int.*, *190*, 1464–1482, doi:10.1111/j.1365-246X.2012.05557.x.

Williams, S. D. P., P. Moore, M. A. King, and P. L. Whitehouse (2014), Revisiting GRACE Antarctic ice mass trends and accelerations considering autocorrelation, *Earth Planet. Sci. Lett.*, *385*, 12–21, doi:10.1016/j.epsl.2013.10.016.

Wouters, B., D. Chambers, and E. J. O. Schrama (2008), GRACE observes small-scale mass loss in Greenland, *Geophys. Res. Lett.*, *35*, L20501, doi:10.1029/2008GL034816.

Wu, X., M. B. Heflin, H. Schotman, B. L. A. Vermeersen, D. Dong, R. S. Gross, E. R. Ivins, A. W. Moore, and S. E. Owen (2010), Simultaneous estimation of global present-day water transport and glacial isostatic adjustment, *Nat. Geosci.*, *3*, 642–646, doi:10.1038/ngeo938.

Yin, J., M. E. Schlesinger, and R. J. Stouffer (2009), Model projections of rapid sea-level rise on the northeast coast of the United States, *Nat. Geosci.*, *2*, 262–266, doi:10.1038/ngeo462.

Yin, J., S. M. Griffies, and R. J. Stouffer (2010), Spatial variability of sea level rise in twenty-first century projections, *J. Clim.*, *23*, 4585–4607, doi:10.1175/2010JCLI3533.1.